Analytical Biochemistry **267,** 1–16 (1999)
Article ID abio.1998.2958, available online at http://www.idealibrary.com on IDEAL®

Measuring Protein Synthesis by Mass Isotopomer Distribution Analysis (MIDA)

Christina Papageorgopoulos,* Kenny Caldwell,*,† Cedric Shackleton,‡ Hans Schweingrubber,§ and Marc K. Hellerstein*,¶

**Department of Nutritional Sciences, University of California at Berkeley, Berkeley, California 94720; ‡Children's Hospital, Oakland, Research Institute, 747 52nd Street, Oakland, California 94609; §Glycomed, 860 Atlantic Avenue, Alameda, California 94501; and ¶Division of Endocrinology and Metabolism, Department of Medicine, SF General Hospital, University of California at San Francisco, 1001 Portrero Avenue, San Francisco, California 94110*

Received September 16, 1997

The measurement of protein kinetics by isotopic techniques has been hindered by the long-standing difficulty of accurately measuring the isotope content of the biosynthetic precursor pool (aminoacyl-tRNA in tissues). Mass isotopomer distribution analysis (MIDA) is a stable isotope-mass spectrometric (MS) technique for measuring biosynthetic precursor enrichments from measurements on a polymeric product, based on combinatorial probabilities of labeled and unlabeled monomeric subunits. Proteins contain complex isotopomer patterns as a result of their relatively high molecular mass, however, so that resolution of the individual mass isotopomers in the polymeric product (an analytic requirement for MIDA) is technically difficult. An approach for measuring protein synthesis by MIDA is described and tested here: First, *in vitro*, using a synthetic peptide present in human serum albumin; and then, *in vivo*, for albumin synthetic rate in rats. A peptide contained in human serum albumin (SVVLLLR) and theoretically recoverable from trypsin/chymotrypsin proteolysis was synthesized by solid-phase peptide synthesis using known mixtures of natural abundance and [5,5,5-$^2H_3$]leucine. Additionally, enriched and natural abundance peptides were mixed *in vitro* to simulate *in vivo* biosynthesis and to address problems of instrument accuracy, precision, and data management. The mass isotopomer patterns of the synthetic peptides were analyzed using electrospray ionization (ESI) with both magnetic sector and quadrupole mass analyzers. The resolution of the magnetic sector was superior to that of the quadrupole instrument, but accuracy and precision in the measurement of mass isotopomer abundances and kinetic parameters were comparable and both gave values close to those predicted. Next, rats were infused with [5,5,5-$^2H_3$]leucine intravenously, and a leucine-rich peptide was isolated and purified from trypsin-digested rat serum albumin (RHPDYSVSLLLR, 1456 Da) and then analyzed by ESI-MS using a magnetic sector instrument. Precursor pool enrichments and fractional synthetic rates (0.45 ± 0.03 day^{-1}, $t_{1/2}$ = 1.53 ± 0.09 days) were calculated. Biosynthetic rates of rat serum albumin were congruent with previously published values. In summary, measurement of protein synthesis and precursor pool enrichments by MIDA is technically feasible and practical *in vivo* using proteolytically derived peptides and ESI-MS analysis.

Schoenheimer first recognized the fundamental process of protein turnover more than 50 years ago (1) by use of stable isotope labeling. The use of isotopic tracers remains the most direct way of measuring dynamic biochemical processes such as protein turnover. Typically, labeled amino acids (AA)[1] are administered and incorporation into proteins of interest is measured. Interpretation of isotope incorporation is complex, however, because of cellular AA compartments. The AA-tRNA pool is the precursor from which proteins are synthesized, but there are several potential metabolic

† Deceased.

[1]Abbreviations used: AA, amino acid; MIDA, mass isotopomer distribution analysis; ESI, electrospray ionization; HSA, human serum albumin; RSA, rat serum albumin; FMOC, 9-fluorenylmethoxycarbonyl derivative; TFA, trifluoracetic acid; AMU, atomic mass units; C.V., coefficient of variation; ANOVA, analysis of variance.

0003-2697/99 $30.00

sources of AA-tRNA (extracellular, intracellular, and proteolytically derived free amino acids) (2, 3) that have confounded the use of surrogate pools to represent the true precursor pool.

Accordingly, application of the precursor–product isotopic approach (i.e., comparing label incorporated into protein to label present in the precursor pool) for measuring fractional replacement rate has been problematic (reviewed in Refs. 2–4). The pivotal methodological problem has been how to determine the isotopic content of the true biosynthetic precursor, the AA-tRNA pool. Tissue AA-tRNA enrichments can be directly measured and, in some instances, have proven similar to intracellular free AA enrichments (5). This is often not the case, however (e.g., Refs. 6 and 7). Direct measurement of label in AA-tRNA can itself be questioned for representing the actual precursor pool for synthesis of a particular protein because of possible compartmentation of the AA-tRNA pool for different proteins (8–10).

Mass isotopomer distribution analysis (MIDA) is a technique based on combinatorial probability analysis that has been used to measure the precursor pool enrichment and synthesis of lipid and carbohydrate polymers (11–15). The theoretical basis of MIDA has been presented in detail elsewhere (11). In brief, stable isotope-labeled monomeric precursor units are administered to allow incorporation into a polymer containing at least two repeats of the precursor units. Labeled and unlabeled subunits combine in the polymer, generating a combinatorial pattern that is described by the binomial or multinomial expansion (11, 12). The perturbed mass isotopomer[2] pattern of the polymeric product is compared to the baseline (natural abundance) pattern; each isotopic enrichment in the precursor pool results in a unique perturbation in the isotopomer pattern of the product. These distinctive patterns may be likened to fingerprints, reflecting the unique combination of labeled and unlabeled precursors at different precursor enrichments. An experimentally determined mass isotopomer pattern (measured by mass spectrometry) can then be compared to theoretical patterns calculated for the polymer over a range of precursor enrichments. By identifying a match between experimental and theoretical combinatorial patterns for the polymer of interest, the isotopic enrichment of the precursor pool is uniquely established.

The MIDA approach has some practical as well as theoretical advantages over other techniques for measuring biosynthesis. Estimates of the precursor pool enrichment by MIDA are performed on the polymer itself, thus do not require isolation from tissue of putative precursors. Moreover, functional compartmentation within the precursor pool does not affect MIDA (11) because the precursor units that actually entered each particular polymer are used for the calculation of precursor enrichment in that polymer, regardless of their relationship to other precursor pools or other polymers.

Accordingly, MIDA represents an attractive approach for measuring protein synthesis. So far, only the synthesis of simple homonuclear polymers, such as fatty acids, cholesterol, and glucose, have been measured by the application of MIDA (11–15). The intent of this work is to investigate strategies for applying the MIDA approach to protein synthesis, using serum albumin as a model protein. First, we tested the approach *in vitro,* on a synthetic peptide made from known enrichments of [5,5,5-$^2H_3$]leucine, to address analytic questions (accuracy, precision, data handling, and possible differences between instruments). Next, we tested the method *in vivo,* for the measurement of rat serum albumin (RSA) synthetic rates.

Theoretical Considerations

Determination of protein synthesis by MIDA poses several challenges. The individual mass isotopomers of the product must be analytically resolved and relative abundances accurately quantified for MIDA calculations. One difference from previously studied analytes (e.g., lipids or carbohydrates; Refs. 11–15) is that the molecular weight of most intact proteins is too high for complete resolution of the multiply charged ions generated in electrospray ionization (ESI) spectra. Mass resolution of small proteins or peptides might be possible, however, by using magnetic sector mass analyzers. Alternatively, mass isotopomers of small peptides [singly charged and $<$1000 atomic mass units (amu)] can be resolved by using quadrupole mass analyzers. A second difference from polymers previously studied by MIDA is that proteins are heteronuclear polymers; they are synthesized from twenty different amino acid precursors. Any portion of a protein that contains at least two repeats of the same potentially labeled amino acid can be considered a polymer, however, in terms of combinatorial probabilities. The presence or absence of unlabeled amino acids merely affects the isotopomer pattern of

[2] Mass isotopomers are defined as isotopic isomers of different nominal mass but identical elemental and chemical composition. Thus, molecules that are of identical structure and elemental composition but different mass because of isotopic substitution, and are therefore resolvable by a mass spectrometer, are designated mass isotopomers. The mass isotopomer lowest in mass is represented as M_0 and others are distinguished by their mass differences from M_0 (M_1, M_2, M_3, etc.).

the remainder of the molecule (11), not the combinatorial probabilities of the variably labeled moiety.

Thus, a general strategy for applying MIDA to proteins is to generate from a large protein small peptides that contain repeats of a selected amino acid. The kinetics of a peptide component represent the kinetics of the intact protein because proteins are synthesized at a single time and the mature protein is not remodeled once synthesized (16). Any peptide isolated from the protein will therefore represent the turnover of the whole molecule.

Serum albumin was selected as a model protein. Serum albumin is accessible, relatively easy to isolate, and has been extensively studied kinetically in humans and animal models. Our experimental strategy was first to identify a peptide from serum albumin with the following characteristics: (a) it can be isolated by enzymatic digestion of albumin, (b) its mass is within a range that allows resolution of its individual mass isotopomers by both magnetic sector and quadrupole mass analyzers, and (c) it contains several repeats of leucine and can thus be considered a polymeric product for combinatorial analysis; second, to synthesize this peptide *in vitro* from labeled leucine at known enrichments and analyze it by mass spectrometry, to assess analytic constraints, the validity of the MIDA model for proteins, and the technical feasibility of the approach for measuring protein turnover; and, third, to apply an analogous strategy for measuring the synthesis rate of serum albumin *in vivo* in the rat.

Identification of Peptides from Human Serum Albumin (HSA)

First, an appropriate peptide was identified. The amino acid sequence of HSA (45) was imported into a computer program (General Protein Mass Analysis for Windows, Version 2.12; Odense SV, Denmark) that facilitates sequence manipulation and then was subjected to simulated enzyme digestions. We looked for leucine-rich peptides because leucine is relatively abundant in albumin (as well as other proteins) and stable isotope-labeled leucine is commercially available and relatively inexpensive. Several peptides of potential interest were identified in a theoretical trypsin/chymotrypsin digestion map. A selected list of computer-generated peptides with their respective average masses and positions in the protein sequence is shown (Table 1). The C-terminal peptide (**L**AVASQAA**LGL**) was a potential candidate peptide since it contains three leucines and has a relatively low mass. A smaller peptide with the sequence SVV**LLL**R was especially attractive since it is both leucine-rich and its mass as the singly charged ion is within the range of both quadrupole and magnetic sector mass analyzers. This latter peptide was chosen for further study.

TABLE 1

Peptides Generated by Computer-Simulated Enzymatic Digestion of HSA

Fragment	MH^+ (ave)	Sequence
7–13	592.75	ISLLF
118–122	658.69	OEPER
29–34	698.75	SEVAHR
89–94	717.84	SLHTLF
366–372	*800.3*	*SVVLLLR***
37–43	823.83	DLGEENF
470–476	828.93	MPCAEDY
131–138	940.99	DDNPNLPR
66–73	951.06	LVNEVTEF
500–508	969.07	TECCOAADK
550–558	1001.21	OTALVELVK
599–609	*1014.21*	*LAVASOAALGL*
534–543	1117.26	HADICTLSEK

Note. Selected peptides generated by computer-simulated digestion of human serum albumin using trypsin and chymotrypsin are shown. Two peptides with repeats of leucine are italicized and underlined.

Identification of Peptides from Rat Serum Albumin (RSA)

RSA has a different AA composition and sequence than HSA; a different peptide than SVVLLLR had to be identified. Based on a simulated trypsin digestion of RSA, the fragment representing AA 361–372 (RHPDYSVSLLLR, 1456.7 Da) contains three leucine repeats, as do two other peptides (including AA362-372 and AA45-57, GLVLIAFSQYLQK, average mass, 1480.8 Da). The 1457-Da peptide could be isolated by HPLC from a trypsin hydrolysate of RSA (see below) and was used for subsequent studies.

METHODS

In Vitro Synthesis of SVVLLLR from Natural Abundance and $^2H_3$-Enriched Leucine

We synthesized the SVVLLLR peptide *in vitro* from mixtures of natural abundance and 5,5,5-$^2H_3$-enriched leucine for use as analytical standards. A solid-phase peptide synthesizer (Applied Biosystems Model 431A; Perkin–Elmer, Foster City, CA) was used to synthesize SVVLLLR from natural abundance leucine, an 8% mixture or a 16% mixture (mole:mole) of 5,5,5-$^2H_3$-enriched leucine (Cambridge Isotope Laboratories, Andover, MA; or Isotec, Miamisburg, OH) and natural abundance leucine. Preparations of natural abundance with or without enriched leucine were first converted to the 9-fluorenylmethoxycarbonyl derivative (FMOC; Bachem,

Torrance, CA) and then used in place of the standard FMOC-leucine during the synthetic cycle (46). The crude SVVLLLR product was applied to a reverse phase C18 column (Model 214TP54, 0.46 × 25 cm, 5 μm pore size; Vydac, Hesperia, CA). A linear gradient of 10 to 50% acetonitrile in water and 0.1% trifluoroacetic acid (Pierce, Rockford, IL) over a period of 45 min was used to separate the SVVLLLR peptide from minor by-products. The flow rate was 1.0 ml/min, and the elution of peptides was monitored by their absorbance at 210 nm. The purified SVVLLLR peptide was collected, lyophilized, and used for mass spectrometric analysis.

Mixtures of Natural Abundance and Isotopically Enriched Peptides

To simulate *in vivo* synthesis and to evaluate the practicality of measuring fractional synthesis by MIDA, mixtures of the purified natural abundance and 16% 5,5,5-$^2H_3$-enriched leucine peptides were prepared. The mixtures were prepared by combining the natural abundance and 16% 5,5,5-$^2H_3$-enriched leucine peptides in the following ratios; 1 part to 3 parts, 1 part to 1 part, and 3 parts to 1 part; in order to simulate 75, 50, and 25% fractional synthesis, respectively.

Animal Studies and Design

Male Sprague–Dawley rats with an average weight of 290 g (range, 250–330 g) were housed in individual cages and maintained on a 12-h light, 12-h dark cycle. A day before tracer infusion, an indwelling catheter was surgically placed into the jugular vein of anaesthetized rats. The rats were allowed to recover for a day following the surgical procedure. On the day of the infusion, a sodium acetate buffered saline solution of [5,5,5-$^2H_3$]leucine (99% enriched) was delivered via the jugular catheter using a minipump at a rate ~50 mg/kg/h for 24 h. The rats were fed *ad libitum* (Purina rat chow). Prior to halting the infusion, a sample of liver tissue for AA-tRNA preparation was collected from rats anaesthetized by phenobarbitol. The abdomen was entered surgically and a section of liver was freeze-clamped *in situ* with Wallenberg clamps precooled in liquid nitrogen. This tissue sample was immersed in liquid nitrogen and subsequently stored at −80°C. A blood sample was also collected into a heparinized syringe from the rats by heart puncture and immediately centrifuged at 2000 rpm for 10 min in a Beckman Model TJ-6 centrifuge (Beckman Instruments, Palo Alto, CA). The plasma was stored at −20°C until further analysis. The rats were killed with a lethal dose of anesthesia following sample collection. All procedures were carried out with the approval of the Office of Laboratory Animal Care of the University of California at Berkeley.

Isolation of RSA from Rat Blood

RSA was isolated to partial purity from rat plasma by modification of the method of Korner (38). To 0.25 ml plasma, a 0.5-ml volume of 10% trichloroacetic acid (w/v) was added to precipitate plasma proteins. The slurry was centrifuged at 2000*g* for 10 min and all but a drop of the supernatant was discarded by decanting. Ice-cold absolute ethanol (1.0 ml) was added to the pellet. The mixture was vortexed vigorously and then centrifuged at 2000*g* for 10 min. The supernatant containing albumin was harvested, dialyzed against distilled water overnight and then lyophilized. Using this isolation protocol, we prepared on average 11.5 mg of protein from 0.25 ml of plasma. This preparation was analyzed by SDS–PAGE (Fig. 4).

Trypsinization of RSA

Lyophilized RSA (20 nmol) was denatured in 25 μl of 6M guanidine–hydrochloride (GuHCl) in 0.4 M ammonium carbonate buffer (pH 8.0). To ensure complete reduction of the 17 disulfide bonds per molecule of albumin, an excess (30 μl) of 45 mM dithiothreitol was added to the protein solution and the mixture was incubated at 50°C for 15 min. When the reaction mixture cooled to room temperature, the reduced cysteine residues were "capped" to prevent reformation of disulfide bonds by the addition of 30 μl of 100 mM iodoacetamide and incubation in the dark for 15 min. The resultant solution was diluted approximately eightfold by the addition of distilled water to reduce the concentration of the GuHCl and incubated with trypsin (enzyme:substrate, 1:25, mole:mole) overnight at 37°C. The digestion was stopped by adjusting the pH to 2 by the addition of a small volume (~5 μl) of glacial acetic acid. The digestion mixture was filtered using Gelman Nylon Acrodisc, 13-mm-diameter, 0.45-μm-pore size syringe filters (Fisher Scientific, Fair Lawn, NJ) in preparation for HPLC analysis.

Identification and Isolation of Leucine-Rich (RHPDYSVSLLLR) Peptide by HPLC

A Beckman HPLC system (Beckman Instruments, Palo Alto, CA) equipped with two pumps (Beckman 110B Solvent Delivery Modules), a variable wavelength detector, and a Shimadzu CR601 Chromatopac integrator (Columbia, MD) was used to separate the tryptic digestion peptides. About 10 nmol of the digestion mixture was injected via a 200-μl injection loop into a C18 reverse phase column (0.46 × 25 cm particle size, 5 μm; Vydac). The sol-

vent system used for chromatography was buffer A, 0.1% (v/v) trifluroacetic acid (TFA, Pierce) in water, pH 2, and buffer B, 0.1% (v/v) TFA in acetonitrile, pH 2. The peptides were separated using a linear gradient of buffer B (0–50% B in 45 min) at a flow rate of 1.0 ml/min and monitored by their absorption at 210 nm. Initially, in order to identify at least one of the leucine-rich candidate peptides, we isolated an RSA sample from the plasma of rats that had not been infused with tracer, digested it with trypsin and separated its tryptic fragments by HPLC. All the peaks were collected and the average mass of each peak was measured by ESI/MS (see below) to identify candidate peptides. RHPDYSVSLLLR was the only leucine-rich peptide that we identified in this manner.

The peptides from HPLC peaks collected off-line were subsequently identified by ESI/MS using a quadrupole mass analyzer (VG Bio-Q mass spectrometer; Micromass, Atrincham, UK) equipped with an electrospray source. About 2 nmol (~5 μl) of sample was injected directly into the source via a Rheodyne 7725 10-μl injector (Cotati, CA). The flow rate of the solvent (50% acetonitrile, 0.1% TFA in water) was 4 μl/min and the ion energy was 1.5 eV. Mass to charge ratio was monitored over a wide mass range (200–1800 amu). Initially, all of the peptides generated by trypsin digestion of RSA were analyzed for mass to charge ratios. Thereafter, the identity of the candidate peptide (RHPDYSVSLLLR) was confirmed by its mass to charge ratio.

Mass Spectrometric Analyses

Quadrupole data for SVVLLLR were obtained using a VG Bio-Q mass spectrometer (Micromass) equipped with an ESI source. About 2 nmol (~5 μl) of sample was injected directly into the source via a Rheodyne 7725 10-μl injector. The flow rate of the solvent (50% acetonitrile, 0.1% TFA in water) was 4 μl/min and the ion energy was 1.5 eV. The needle voltage was between 3.0 and 3.8 kV and the multiplier voltage was between 700 and 750 V. Mass spectral profiles of the isotopomers were obtained by acquiring a narrow scan over the mass region of the protonated molecule $[M + H]+$; centroid m/z 799.6. Individual samples were run in triplicate.

Magnetic sector data were acquired using a Finnigan MAT900 mass spectrometer (Finnigan MAT, Bremen, Germany), a double focusing magnetic sector instrument (E-B type) equipped with a 20 kV conversion dynode/SEM point detector, and an array-type focal plane detector (PATRIC). The Finnigan MAT ESI interface (API) was used in the positive mode. Droplet desolvation was accomplished in the heated capillary and by collisional processes in the ESI interface. Samples were dissolved in 50% acetonitrile in water and a 10–20 pmol/μl solution was infused into the ESI interface via a Harvard Apparatus Syringe Infusion Pump 22 (South Natick, MA) at flow rates of 1.5–3 μl/min. Spectra were acquired in profile mode using ESCAN (electric scans) at 500 or 1000 s/decade over a narrow mass range. The resolution was adjusted to get baseline resolved isotope clusters for the molecular ions of interest. Up to 300 scans were accumulated to acquire a good average of the isotope distribution. All samples were run under similar conditions.

Data Handling

The optimal peak integration approach to achieve maximal accuracy and precision of mass isotopomer abundance measurements has not been established. We imported the mass profile data of natural abundance, 8 and 16% 5,5,5-$^2H_3$-enriched leucine, and mixtures of peptides generated by the magnetic sector or quadrupole instruments into a curve-fitting software package available from Microcal Software, Inc. (Origin, Version 3.73, Peak Fitting Module; Northampton, MA). The M_0 through M_4 isotopomers of the natural abundance peptide and the M_0 through M_8 isotopomers of the peptides synthesized from stable isotopically labeled leucine were fitted. Several of the curve-fitting modalities available with this package were compared. The curve fits were evaluated on the basis of both their statistical fit to the primary data points and the correspondence of the fitted baseline pattern to the theoretically calculated baseline (natural abundance) pattern predicted to be present.

MIDA Calculations

The abundances of the M_0, M_3, and M_6 isotopomers change most dramatically as a result of isotope incorporation from [5,5,5-$^2H_3$]leucine. Accordingly, it is sometimes preferable analytically to exclude the other less abundant mass isotopomers from quantitation (to maximize dwell time on the most higly labeled ions and to reduce potential analytic error due to the lower signal-to-noise present in the other masses). When this is done, the curve-fitted abundances of the M_0, M_3, and M_6 isotopomers are converted to fractional abundances by dividing each peak area by the total (i.e., $(M_0)/(M_0 + M_3 + M_6)$). The theoretical combinatorial probabilities used for calculating biosynthetic parameters (15) were also normalized to the sum of $M_0 + M_3 + M_6$ and calculated in the same manner. Whether a complete or incomplete ion spectrum was monitored, the fractional abundances of each mass isotopomer in the

TABLE 2

Theoretical Mass Isotopomer Abundances and Derived Parameters for Peptide SVVLLLR Synthesized from $^2H_3$-Labeled Leucine at Different Precursor Enrichments

	A. Mass isotopomer abundances (M_x)						
p (%)	M_0 799.5	M_1 800.5	M_2 801.5	M_3 802.5	M_4 803.5	M_5 804.5	M_6 805.5
0	0.6221	0.2853	0.0754	0.0146	0.0023	0.0003	0.0000
5	0.5333	0.2446	0.0647	0.0968	0.0405	0.0105	0.0064
10	0.4535	0.2080	0.0550	0.1619	0.0709	0.0185	0.0204
15	0.3820	0.1752	0.0463	0.2113	0.0941	0.0247	0.0405
20	0.3185	0.1461	0.0386	0.2465	0.1107	0.0291	0.0654
25	0.2624	0.1204	0.0318	0.2687	0.1213	0.0319	0.0937
30	0.2134	0.0979	0.0259	0.2795	0.1265	0.0333	0.1241

	B. Normalized abundances			C. Excess abundances (ΔA^*_x)			
	M_0	M_3	M_6	ΔA^*_0	ΔA^*_3	ΔA^*_6	$\Delta A^*_6/\Delta A^*_3$
0	0.9770	0.0229	0.0001	0.0000	0.0000	0.0000	
5	0.8379	0.1520	0.0101	−0.1392	0.1291	0.0101	0.0779
10	0.7133	0.2546	0.0321	−0.2637	0.2317	0.0320	0.1381
15	0.6027	0.3334	0.0639	−0.3743	0.3105	0.0638	0.2056
20	0.5053	0.3910	0.1037	−0.4717	0.3681	0.1037	0.2817
25	0.4200	0.4300	0.1500	−0.5570	0.4071	0.1499	0.3683
30	0.3458	0.4530	0.2012	−0.6312	0.4301	0.2011	0.4677

Note. Best fit regression equation for p as function of $\Delta A^*_6/\Delta A^*_3$ ratio: $p = -0.0239 + 1.0236 \cdot (\Delta A^*_6/\Delta A^*_3) - 1.0414 \cdot (\Delta A^*_6/\Delta A^*_3)^2 + 1.0160 \cdot (\Delta A^*_6/\Delta A^*_3)^3 - 0.8232 \cdot (\Delta A^*_6/\Delta A^*_3)^4 + 0.3783 \cdot (\Delta A^*_6/\Delta A^*_3)^5$). Best fit regression equation for ΔA^*_3 as function of p (if all ions are included): $\Delta A^*_3 = 1.8234 \cdot (p) - 3.6940 \cdot (p)^2 + 2.0276 \cdot (p)^3 + 1.0549 \cdot (p)^4 - 1.7611 \cdot (p)^5$. If only M_0, M_3, and M_6 are included in the measured ions, the correction equation is used (17 and see Appendix). Normalized abundances are calculated as described in the text, by dividing each mass isotopomer fractional abundance by the sum of the fractional abundances sampled. Excess abundances were calculated by subtracting the normalized abundances of each mass isotopomer in the natural abundance peptide (see text).

natural abundance peptide were subtracted from their abundances in the 8%-enriched and 16%-enriched peptides to determine excess mass isotopomer abundances (ΔA_0, ΔA_3, and ΔA_6, also termed EM_0, EM_3, and EM_6) (11). A computer algorithm (11, 17) was used to generate the theoretical mass isotopomer abundances expected for the SVVLLLR peptide over a range (0–30%) of [$^2H_3$]leucine precursor enrichments (Table 2A). The M_0, M_3, and M_6 isotopomer abundances of the theoretical data set were normalized to the sum of $M_0 + M_3 + M_6$ abundances (Table 2B), and unlabeled abundances were subtracted to calculate excess isotopomer abundances (Table 2C). The ratio of ΔA_6 to ΔA_3 was plotted against the precursor enrichment and a polynomial equation was fitted to the data. The precursor enrichment for measured samples was inferred from the measured $\Delta A_6/\Delta A_3$ (15) ratio using the resulting regression equation (see note to Table 2A).

For *in vivo* calculations of biosynthetic precursor pool enrichments, the normalized abundances of the natural abundance peptide, isolated from the RSA of a rat that had not been infused with labeled leucine, were subtracted from those of enriched peptides to determine excess isotopomer abundances (ΔA_0, ΔA_3, and ΔA_6). A computer algorithm (11, 17) was used to generate theoretical isotopomer abundances for the RHPDYSVSLLLR peptide over the range (0–60%) of precursor pool enrichments (Table 3A). The M_0, M_3, and M_6 isotopomer abundances for the theoretical data set were normalized in the same manner (Table 3B) as that for the measured results and the theoretical excess isotopomer abundances were calculated (Table 3C). The ratio of ΔA_6 to ΔA_3 was plotted against the precursor enrichment (Fig. 3) and a polynomial equation was fitted to the data (see note to Table 3), as described above. The precursor enrichment (p) was determined from the measured $\Delta A_6/\Delta A_3$ ratio using this equation (see note to Table 3).

Calculation of Fractional Synthesis

Determination of fractional synthesis of protein by the precursor–product approach is a two-step process (11): First, the isotopic labeling pattern of newly synthesized protein molecules is determined, and then the isotopic incorporation in the mixture of molecules in the sampled pool is compared, to establish dilution by

TABLE 3

Theoretical Abundances and Excess Abundances of Mass Isotopomers M_0 through M_6 for the RSA Peptide (RHPDYSVSLLLR)

	A. Mass isotopomer abundances						
p (%)	M_0 1454.8	M_1 1455.8	M_2 1456.8	M_3 1457.8	M_4 1458.8	M_5 1459.8	M_6 1460.8
0	0.4295	0.3489	0.1558	0.0498	0.0127	0.0027	0.0005
5	0.3682	0.2992	0.1336	0.1009	0.0581	0.0234	0.0102
10	0.3131	0.2544	0.1136	0.1407	0.0940	0.0398	0.0241
15	0.2638	0.2143	0.0957	0.1703	0.1212	0.0523	0.0412
20	0.2199	0.1787	0.0798	0.1905	0.1405	0.0612	0.0606
25	0.1812	0.1472	0.0657	0.2023	0.1525	0.0668	0.0817
30	0.1473	0.1197	0.0534	0.2066	0.1582	0.0696	0.1034
35	0.1179	0.0958	0.0428	0.2043	0.1583	0.0698	0.1249
40	0.0928	0.0754	0.0337	0.1964	0.1535	0.0679	0.1454
45	0.0715	0.0581	0.0259	0.1838	0.1446	0.0640	0.1640
50	0.0537	0.0436	0.0195	0.1674	0.1324	0.0587	0.1799
55	0.0391	0.0318	0.0142	0.1481	0.1177	0.0523	0.1922
60	0.0275	0.0223	0.0100	0.1269	0.1013	0.0450	0.2001

	B. Normalized abundances			C. Excess isotopomer abundances (ΔA^*_x)			
	M_0	M_3	M_6	ΔA^*_0	ΔA^*_3	ΔA^*_6	$\Delta A^*_6/\Delta A^*_3$
0	0.8951	0.1038	0.0010	0.0000	0.0000	0.0000	
5	0.7682	0.2105	0.0213	−0.1269	0.1066	0.0203	0.1904
10	0.6552	0.2945	0.0504	−0.2400	0.1907	0.0493	0.2587
15	0.5550	0.3584	0.0866	−0.3401	0.2545	0.0856	0.3361
20	0.4668	0.4044	0.1287	−0.4283	0.3006	0.1277	0.4248
25	0.3895	0.4349	0.1756	−0.5056	0.3311	0.1745	0.5271
30	0.3222	0.4518	0.2261	−0.5730	0.3479	0.2250	0.6467
35	0.2638	0.4569	0.2793	−0.6314	0.3531	0.2783	0.7882
40	0.2135	0.4519	0.3346	−0.6817	0.3481	0.3336	0.9583
45	0.1704	0.4383	0.3913	−0.7247	0.3345	0.3902	1.1667
50	0.1339	0.4174	0.4487	−0.7612	0.3135	0.4477	1.4278
55	0.1031	0.3903	0.5066	−0.7920	0.2865	0.5055	1.7647
60	0.0775	0.3581	0.5644	−0.8176	0.2542	0.5633	2.2158

Note. Best fit regression equation for p vs $\Delta A^*_6/\Delta A^*_3$ ratio: $p = -1.2875 + 1.1255 \cdot (\Delta A^*_6/\Delta A^*_3) - 1.1461 \cdot (\Delta A^*_6/\Delta A^*_3)^2 + 0.93860 \cdot (\Delta A^*_6/\Delta A^*_3)^3 - 0.5013 \cdot (\Delta A^*_6/\Delta A^*_3)^4 + 0.1229 \cdot (\Delta A^*_6/\Delta A^*_3)^5$. The best fit regression equation for ΔA^*_3 as a function of p (if all mass isotopomers are included): $\Delta A^*_3 = 1.1390 \cdot (p) - 2.4175 \cdot (p)^2 + 1.5260 \cdot (p)^3 + 0.2120 \cdot (p)^4 - 0.7717 \cdot (p)^5$. In an incomplete ion spectrum is monitored or included in the calculation (e.g., M_0, M_3, and M_6), the correction equation is applied (17 and see Appendix).

unlabeled molecules. Label in newly synthesized molecules is a function of the isotope content of the precursor (p); accordingly, p is first determined and the incorporation of labeled amino acids into protein is then compared. The fractional synthesis (f) or the proportion of newly synthesized molecules present in the pool is represented by the quotient of the enrichment in the sampled pool to the enrichment in newly synthesized molecules for a traditional two-pool, precursor–product model

$$f = \Delta A(t)/\Delta A_\infty,$$

where $\Delta A(t)$ is the measured enrichment in the mixture, sampled at time t; ΔA_∞ is the enrichment at plateau, or the precursor enrichment in a one-source biosynthetic system; and $\Delta A(t) = \Delta A_\infty(1 - e^{-k_s t})$. Applying this to albumin synthesis from [$^2H_3$]leucine and using our nomenclature (11–15, 17)

$$f = \Delta A_3(\text{mixture})/\Delta A^*_3 = 1 - e^{-k_s t}, \qquad [1]$$

where ΔA_3 (mixture) represents the measured enrichment of the M_3 isotopomer in the mixed pool sampled and ΔA^*_3 represents the plateau or asymptotic ΔA_3 (mixture) enrichment at $t = \infty$. ΔA^*_3 and p are calculated using the equations in the notes to Tables 2 (for HSA) and 3 (for RSA). A correction equation is used for calculating f when the ion spectrum sampled is incom-

plete, i.e., when only M_0, M_3, and M_6 isotopomers were quantified (see appendix).

The fractional synthetic rate constant (k_s) is calculated as follows (1), in timed physiologic experiments (see below)

$$k_s = -\ln(1 - f)/t. \quad [2]$$

The derivation and theoretical aspects of these calculations have been presented elsewhere in detail (11, 12, 14, 17).

Statistical Analyses

The kinetic values for RSA from the two groups of rats were compared by applying one-factor ANOVA. The enrichments of plasma leucine, leucyl-tRNA, and that calculated by MIDA were analyzed by repeated measures ANOVA. Standard deviations of parameter estimates were compared using an F test for equal variances.

RESULTS

In Vitro Studies

HPLC and mass spectrum of SVVLLLR peptide synthesized in vitro. The SVVLLLR peptide was separated from other by-products of the *in vitro* synthesis by using an acetonitrile gradient on a reverse-phase C18 column. Under these conditions, the SVVLLLR peptide elutes at 20 min (Fig. 1). The mass spectrum of the eluant was then analyzed using the VG BioQ quadrupole mass spectrometer (Fig. 1, inset). The major species in the mass spectrum was the singly charged 799.5 ion. Several minor molecular fragments are also observed in the mass spectrum. The 613.3 and 514.3 ions are fragments with the respective sequences VLLLR and LLLR. The 419.3 ion has the sequence SVVL, and the 286.2 ion is a fragment with the sequence SVV. The signal at 401 is the doubly charged ion of the SVVLLLR peptide.

Mass profiles of the SVVLLLR peptide. Representative mass profiles of the singly charged SVVLLLR peptide collected from the magnetic sector instrument (Fig. 2A) and the quadrupole instrument (Fig. 2B are shown. The profile of the peptide synthesized from natural abundance leucine is displayed in the top panel of both figures, that of the peptide synthesized from 8% 5,5,5-$^2H_3$-enriched leucine is displayed in the middle panel, and that of the peptide synthesized from 16% 5,5,5-$^2H_3$-enriched leucine is displayed in the bottom panel. M_0 is the most abundant isotopomer, with a mass 799.5; 800.5, 801.5, 802.5, 803.5, 804.5, 805.5, 806.5, and 807.5 are M_1, M_2, M_3, M_4, M_5, M_6, M_7, and M_8 isotopomers, respectively. The difference in resolution between the magnetic sector and quadrupole mass analyzers is evident: The isotopomers of the peptides collected on the magnetic sector are baseline resolved, whereas those collected on the quadrupole are not. In both sets of mass profile data, the abundances of the M_3 and M_6 isotopomers increase as the enrichment of the $^2H_3$-enriched leucine precursor increases, as expected from theoretical calculations (Table 2C). The mass profiles of mixtures of enriched and natural abundance peptides, using the quadrupole instrument, are shown (Fig. 2C). These mixtures were formed by combining different proportions of the natural abundance unenriched peptide with the peptide synthesized from 16% 5,5,5-$^2H_3$-enriched leucine, to simulate *in vivo* synthesis. In the top panel, fractional synthesis (f) is 75% (i.e., 75% of SVVLLLR molecules are from the enriched pool and 25% from the natural abundance pool), in the middle panel f is 50%, and in the bottom panel f is 25%.

Curve-fitting of mass profiles. The mass profiles of peptides were imported into a curve-fitting program and various fitting options were tested. The imported data were fitted by different functions (e.g., Gaussian, Voigt, and Lorenz), a baseline was tested to fit unresolved data, and the width of each curve was kept constant or allowed to vary. The curve-fitting strategies were evaluated by closeness of observed to expected mass isotopomer abundances of the native peptide.

Magnetic sector instrument. Since the magnetic sector-derived isotopomer patterns were already baseline-resolved, fitting a baseline to the data was not necessary. Mass isotopomer peaks are different from chromatographic peaks in that peak width does not vary with concentration, so widths of the individual peaks were not allowed to vary but rather kept the same in the fitting procedure. The percentage of error [(observed − theoretical)/(theoretical) × 100] increased as the abundances of the isotopomers decreased. Although these curve-fitting strategies gave comparable results, the data were somewhat better characterized by the Gaussian function (not shown). Mass profiles acquired with the magnetic sector instrument were therefore fitted using the Gaussian function.

Quadrupole instrument. The data collected using the quadrupole mass analyzer were also fitted with Gaussian and Voigt functions, but in this case only M_0 through the M_3 could be fitted with confidence. Furthermore, due to the lack of baseline resolution, a best fit baseline was allowed to be selected by the program. As with the magnetic sector data set, the widths of the individual curves were held constant for all mass isotopomers. The statistical correlation of the Voigt fit (R^2 = 0.998) was similar that of the Gaussian fit (R^2 =

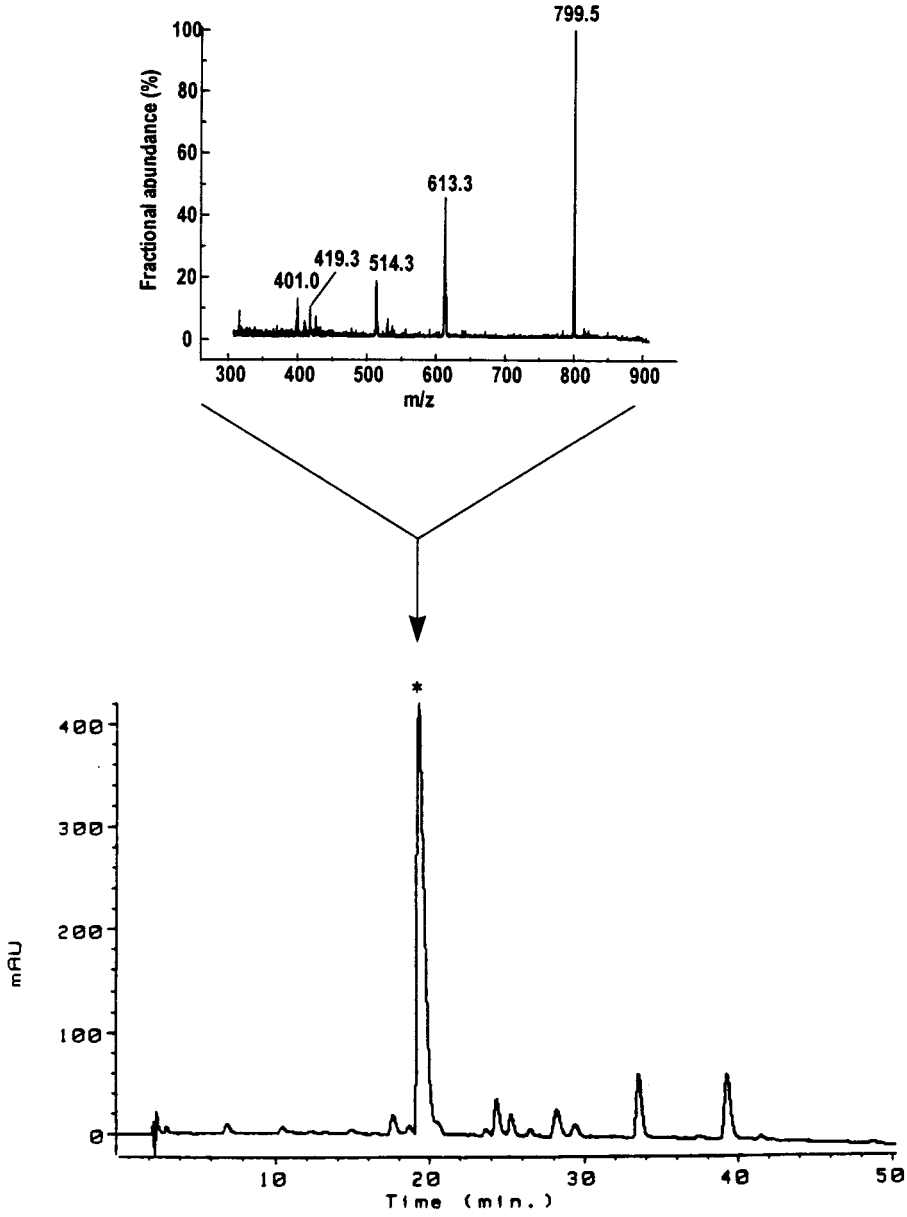

FIG. 1. HPLC isolation and subsequent ESI/mass spectrometric identification of the SVVLLLR peptide. (Inset) The spectrum collected by the VG BioQ quadrupole mass analyzer of the purified SVVLLLR peptide (peak collection from HPLC was baseline-to-baseline).

0.996). The percentage of errors for the M_0, M_1, and M_2 were about twofold higher for the Voigt fits versus the Gaussian fits and comparable for the M_3, but the Voigt appeared to better represent the raw data points by visual inspection (not shown). Based on this observation, the Voigt function was used to fit the quadrupole-generated data sets.

Calculation of precursor enrichments from fitted mass profiles. The mass profiles of the SVVLLLR peptides synthesized from 8 and 16% 5,5,5-$^2H_3$-enriched leucine were curve-fitted according to the selected strategies discussed in the previous section. The theoretical MIDA table was then applied (Table 2) to calculate precursor enrichment and fractional synthesis (f) for these enriched peptides. In Table 4 the measured values are compared to the expected values. The precursor enrichments calculated from the magnetic sector and quadrupole mass profiles of the 8% 5,5,5-$^2H_3$-enriched leucine peptides were 7.65 and 7.87%, respectively. For the 16% peptide, precursor enrichments were 16.02 and 15.71%, respectively. The expected f for both peptides was 100% since this set of

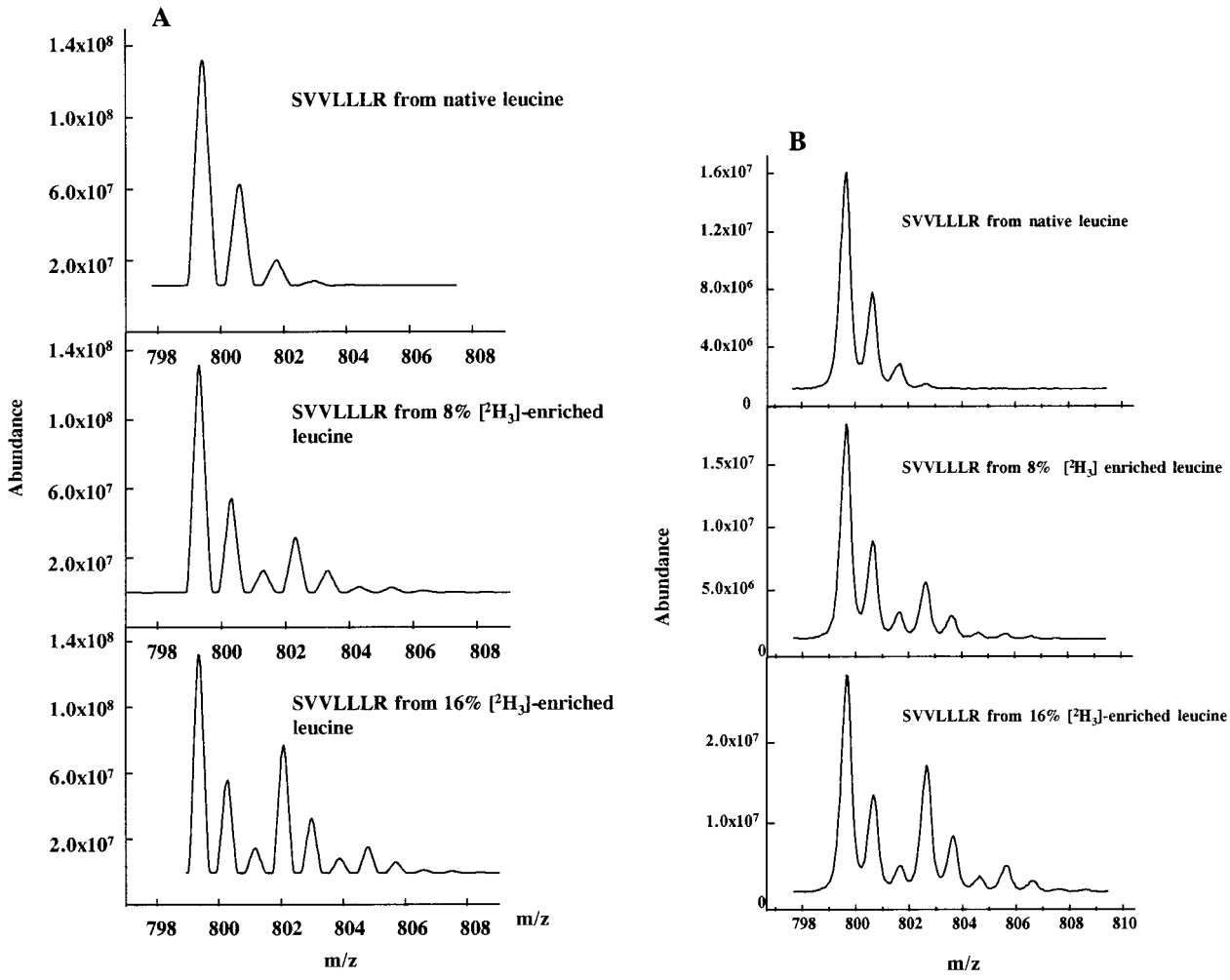

FIG. 2. (A) Mass profiles of the SVVLLLR peptides synthesized from 0, 8, and 16% enriched [$^2H_3$]leucine collected from the magnetic sector mass analyzer. (B) Mass profiles of the SVVLLLR peptides synthesized from 0, 8, and 16% enriched [$^2H_3$]leucine collected from the quadrupole mass analyzer. (C) Mass profiles of the SVVLLLR peptide mixtures collected from the quadrupole mass analyzer.

peptides was not mixed with natural abundance peptide. The measured values of *f* and percentage of error in their measurement were close to the expected 100% value.

Analysis of mixtures of enriched and unenriched peptides. To simulate *in vivo* biosynthesis, mass profiles of the mixture of native and 16% 5,5,5-$^2H_3$-enriched leucine peptides were analyzed using the quadrupole mass analyzer, according to the peak-fitting strategy described above. The results of this analysis are listed in Table 5. The mixtures simulated 25, 50, 75, and 100% *f*, but the expected precursor enrichment in all of the mixtures was 16%. The measured values of *f* measured were 21, 46.6, 77.1, and 101.4%; the precursor enrichments measured were 17.6, 16.5, 15.4, and 15.7%, respectively.

Precision and accuracy of quadrupole and magnetic sector instruments. To assess the precision of the instruments, standard deviation and coefficients of variation of the measured and normalized isotopomers abundances, precursor enrichments, and *f* measurements were compared. Measurements obtained on both instruments had similar coefficients of variation (no significant difference in variances by *F* test).

In Vivo Studies

Isolation and purification of RSA and identification and isolation of the leucine-rich tryptic peptide. Analysis of the RSA preparation by SDS–PAGE indicated that it consisted of one band with the same electrophoretic properties as albumin standard and an approximate molecular weight of 60 kDa (not shown). We

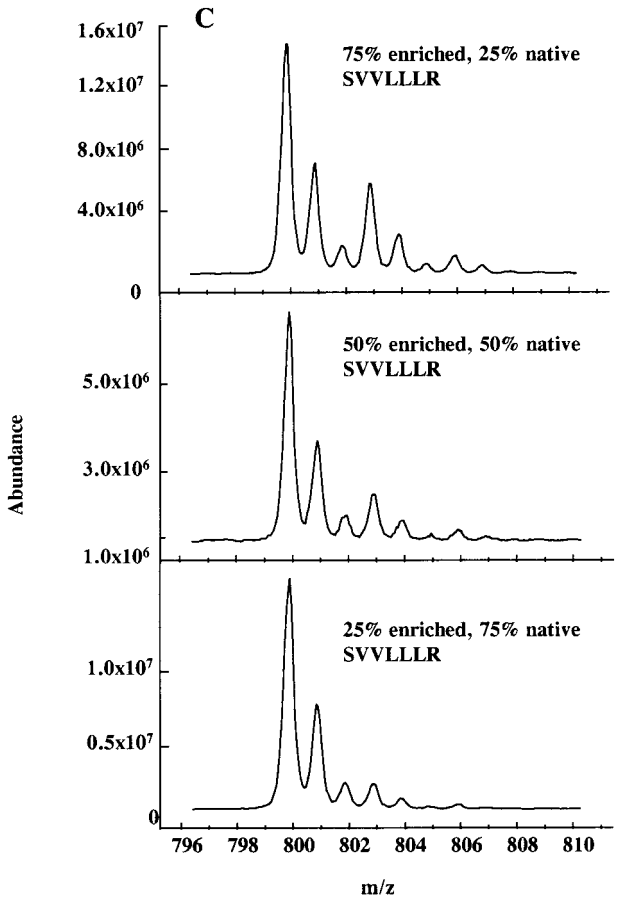

FIG. 2—*Continued*

attempted to prepare a relatively pure RSA to minimize the number of contaminating peptides potentially generated by trypsin digestion. Purity is not as critical a concern for our analysis as it is for classical studies monitoring the incorporation of tracer into protein, however, because the ultimate mass spectrometric measurements are on trypsin-generated peptides that are specific to albumin. Interposition of a subsequent analytic step specific for albumin makes potential contamination by other proteins less problematic.

A typical HPLC profile showing the peptides generated by trypsin digestion of albumin is shown (Fig. 3). The chromatographs were reproducible for individual samples of RSA isolated from different rats (data not shown). One of the candidate peptides (RHPDYSVSLLLR), eluting at 35 min, was identified from the trypsin digest by ESI/MS (Fig. 3) and was chosen to represent the kinetics of RSA. The mass spectrum of this peptide, collected off-line, was analyzed by the quadrupole mass analyzer (Fig. 3). The peptide has several protonation sites on the basic residues; the major ion species that is observed is the double charged ion (m/z = 728.5).

Mass spectrometric analyses of RHPDYSVSLLLR peptide. The mass profiles collected from the magnetic sector instrument of the doubly charged RHPDYSVSLLLR peptide derived from RSA samples are shown (Fig. 4) from a rat that had not received an infusion of tracer (natural abundance) and a rat that received an infusion of [5,5,5-$^2H_3$]leucine (infused). Because we analyzed the doubly charged ion, two peaks are observed per atomic mass unit. The most abundant mass isotopomer is M_0 (m/z 728.25), and 728.75, 729.25, 729.75, 730.25, 730.75, 731.25, 731.75, and 732.25 are the M_1, M_2, M_3, M_4, M_5, M_6, M_7, and M_8 mass isotopomers, respectively. The M_1, M_2, and M_3 mass isotopomers, observed in the natural abundance spectrum, are due to natural abundance ^{13}C (1.1%). Comparison of predicted to measured isotopomer abundances for the natural abundance peptide revealed lower accuracy for the less-abundant isotopomers (5.4, 6.9, and 5.4% error for M_2, M_3, and M_4, respectively) than for the more abundant isotopomers (<3% error for M_0 and M_1). In the enriched sample (Fig. 4), the abundance of the M_3 and M_6 isotopomers increases as a result of [$^2H_3$]leucine incorporation. In addition, M_4, M_5, M_7, and M_8 also increase. This reflects the natural abundance envelope from the remainder of the peptide interacting with the labeled leucine subunits that have been incorporated into the peptide.

TABLE 4

Biosynthetic Parameters Calculated for Labeled SVVLLLR Synthesized *in Vitro*, Using Magnetic Sector and Quadrupole Mass Analyzers

Expected precursor enrichment (%)	Measured precursor enrichment (%)	Deviation (%)	Expected *f* (%)	Measured *f* (%)
		Magnetic sector		
8	7.65	−4.38	100	93.2
16	16.02	0.13	100	100.0
		Quadrupole		
8	7.87	−1.62	100	96.9
16	15.71	−1.81	100	101.2

Note. Precursor enrichment and fractional synthesis determined by isotopomer analysis of SVVLLLR synthesized from 8% and 16% $^2H_3$-enriched leucine. Isotopomer patterns were analyzed using magnetic sector and quadrupole mass analyzers. Deviation was calculated using the following equation: (measured − expected) ÷ (expected) × 100. Expected precursor enrichment refers to the known proportion of $^2H_3$-enriched leucine mixed *in vitro* for the peptide synthesis; *f* is defined in the text (Eq. [1]).

TABLE 5

Simulated "Biosynthetic" Parameters Calculated for Mixtures of Enriched and Natural Abundance SVVLLLR Peptides

Mixed peptide		Expected precursor enrichment	Measured precursor enrichment				
% Native	% 16%	(%)	(%)	% Deviation	Expected *f* (%)	Measured *f* (%)	% Deviation
75	25	16	17.60	10.00	25	21.0	15.9
50	50	16	16.52	3.25	50	46.6	6.8
25	75	16	15.37	−3.91	75	77.1	−2.9
0	100	16	15.65	−2.21	100	101.4	−1.4

Note. Fractional synthesis (*f*, see Eq. [1] in text) and precursor enrichment were determined by mass isotopomer distribution analysis of mixtures of native and 16% $^2H_3$-enriched leucine peptides mixed in different proportions to simulate *in vivo* biosynthesis. Deviation was calculated using the following equation: (measured − expected) ÷ (expected) × 100.

Calculation of biosynthetic parameters (p and f) in vivo. We used the mass profiles to calculate the precursor enrichment (*p*) and fractional synthesis (*f*) of RSA. An RSA-derived sample will be used as an example of the calculation procedure. The Gaussian-fitted data are shown (Table 6A) for a rat that was infused with labeled leucine. The abundances of the M_0, M_3, and M_6 isotopomers are normalized by taking the area under curve of each and dividing by the sum of the areas under the curve of the M_0, M_3, and M_6 isotopomers (i.e., to normalize M_0, divide 31.61% by the sum of 31.61, 8.98, and 4.56%). The fractional abundances calculated for these isotopomers and those of the natural abundance peptide are shown (Table 6B). Next, the excess abundances (ΔA_x) are calculated by subtracting the normalized fractional abundance of each isotopomer in the natural abundance sample from the abundance of the same isotopomer in the enriched sample (Table 6C). The (ΔA_6) value (0.0977) is then divided by the (ΔA_3) value (0.1034) and this ratio (0.944) is used in the best-fit equation to calculate *p*, as described previously (16 and the note to Table 3). The calculated value of *p* (0.396) reflects the enrichment of the biosynthetic precursor of this peptide and thus that of RSA. This value of *p* and the abundance of (ΔA_3) allows calculation of *f* (16 and the note to Table 3). The fractional synthesis rate constant (k_s) is then calculated using Eq. [2]: $f = 0.2924$, $t = 0.09$ days (duration of the infusion), and $k_s = 0.376$ day^{-1}. The $t_{1/2}$ of RSA is $\ln(2)/k$ or $0.693/0.376 = 1.80$ days. Average measurements of *p*, *f*, k_s, and $t_{1/2}$ for rats are shown (Table 7).

Comparison of precursor enrichment determined by MIDA and by AA-tRNA measurements and from plasma leucine. Measurements of the enrichment of plasma leucine, hepatic leucyl-tRNA, and hepatic *p* calculated by MIDA were compared in four rats (Fig. 5). The enrichment of leucine in plasma is not significantly different than that bound to tRNA or the MIDA-calculated *p*. The measurements of plasma leucine and leucyl-tRNA enrichment were highly variable; variability in the values of precursor enrichment (Fig. 5) measured by leucyl-tRNA was higher than that for the values determined by MIDA.

DISCUSSION

MIDA has previously been applied for biosynthetic measurements of small polymers (e.g., fatty acids, cholesterol, and carbohydrates) that can be analyzed using tabletop gas chromatograph/mass spectrometers (11–15). Since analysis of the individual mass isotopomer abundances of most intact proteins is not possible using currently available instruments but MIDA is in many ways a potentially ideal solution to the problem of precursor pool compartmentation that has plagued protein synthesis measurements (2–10), the first part of our overall plan for measuring protein synthesis by MIDA was to analyze small peptides from partial hydrolysates of proteins by quantitative mass spectrometry.

Two different types of mass analyzers (magnetic sector and quadrupole) were used to collect mass profile data of the *in vitro* synthesized (SVVLLLR) peptide. A priori, magnetic sectors possess the advantage of a higher resolution than quadrupole instruments. The greater expense and generally lower availability of sector instruments are disadvantages. Although, the magnetic sector-acquired mass profiles were baseline resolved, whereas those collected on the quadrupole were not, the unresolved data from the quadrupole yielded results comparable to those of the magnetic sector with appropriate peak fitting strategies (Table 4).

To further evaluate the limitations of instrument analysis, the abundance of perturbed mass isotopomers as a function of three factors (*p*, *f*, and polymer length) can be modeled. The fractional abundances of the labeled mass isotopomers (especially M_6) are

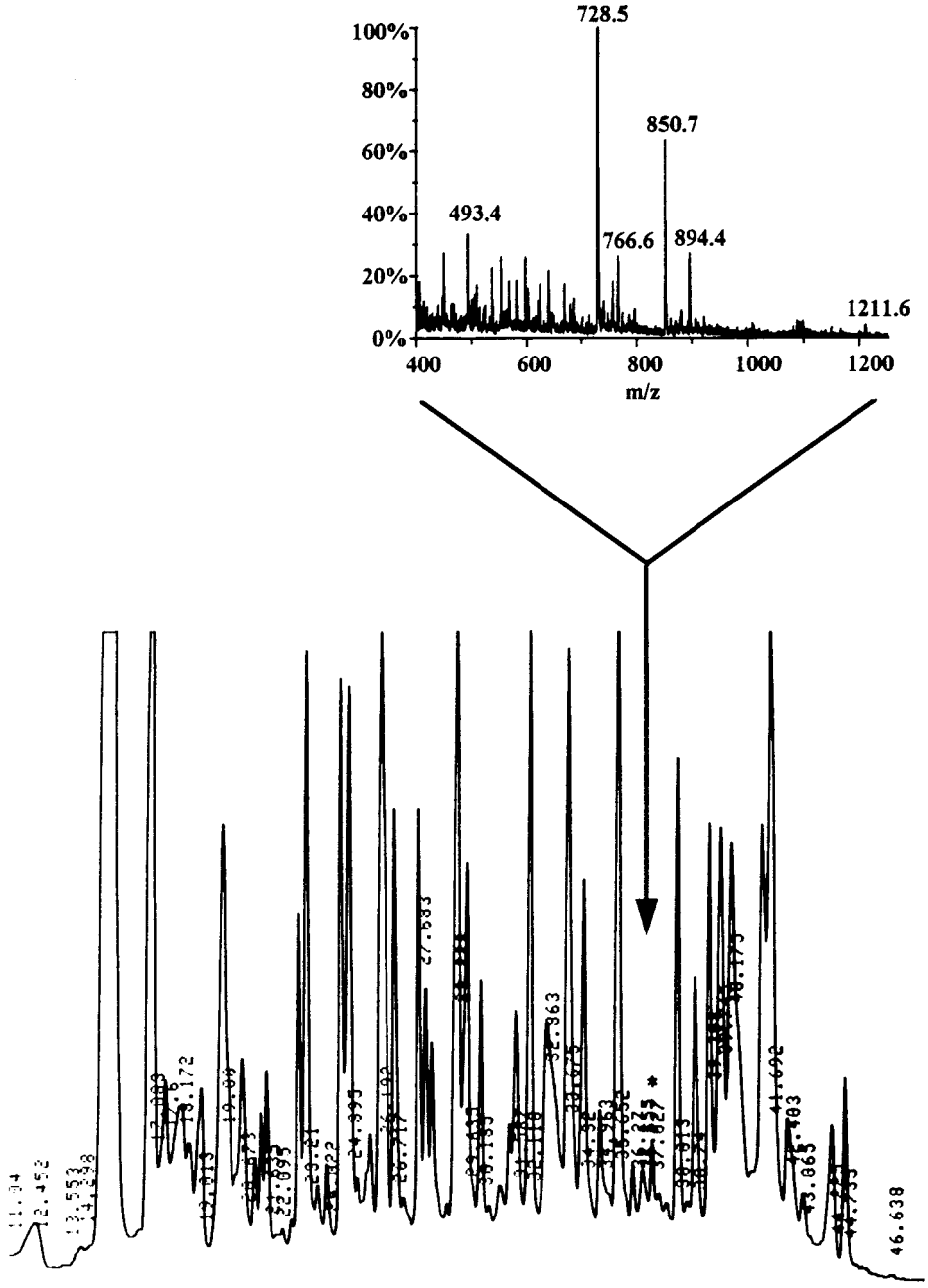

FIG. 3. HPLC isolation and subsequent electrospray/mass spectrometric identification of the RHPDYSVSLLLR peptide. Peak collection from HPLC was from local baseline-to-baseline.

greatly dependent on the length of the polymer as well as the precursor pool enrichment (i.e., an increase in polymer length by one unit nearly doubles the abundance of the M_6 mass isotopomer). The SVVLLLR peptide contains three leucines and similar small peptides containing three repeats of a single amino acid can be derived from other proteins that we have examined thus far (unpublished observations). Even though more repeats than three of an AA are more favorable, they are less frequently found within a small peptide. Larger peptides with many repeats of a single amino acid can be detected, but they tend to be multiply charged, so that resolution of their isotopomer pattern requires mass analysis with a magnetic sector instrument.

Next we applied this approach to the measurement of RSA synthesis *in vivo.* Although precursor pool enrichments were maintained at clearly nontracer levels

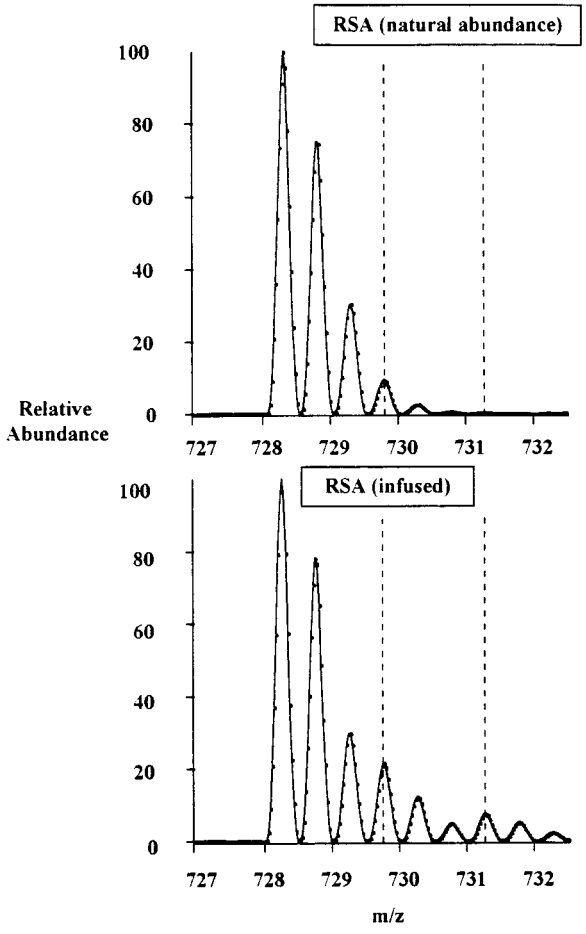

FIG. 4. Mass profiles of the RHPDYSVSLLLR peptide isolated from an unlabeled rat and a rat that was infused with $^2H_3$-labeled leucine.

TABLE 6

Conversion of Measured Mass Isotopomer Abundances of RSA Peptide into ΔA_x Values

(A) Measured mass isotopomer abundances of the enriched peptide (RHPDYSVSLLLR) after labeling *in vivo*

Isotopomer	Area under the curve	Normalized area (%)
M_0	30379527	31.61
M_1	26911317	28.00
M_2	13202056	13.74
M_3	8633228	8.98
M_4	5426532	5.65
M_5	2454522	2.55
M_6	4380195	4.56
M_7	3113702	3.24
M_8	1611353	1.68

(B) Normalized fractional isotopomer abundances of key isotopomers (M_0, M_3, and M_6)

Isotopomer	Normalized isotopomer abundance (enriched peptide)	Normalized isotopomer abundance (natural abundance peptide)
M_0	0.7001	0.9012
M_3	0.1990	0.0955
M_6	0.1009	0.0033

(C) Excess fractional abundances (ΔA_x) of key isotopomers

Isotopomer	Excess abundance (ΔA_x)
M_0	−0.2011
M_3	0.1034
M_6	0.0977

(39%), the synthesis rate of RSA determined by MIDA was 46%/day in *ad libitum* fed rats (Table 7) or a $t_{1/2}$ of 1.53 ± 0.09 days. These values are consistent with several previously published estimates (25, 33, 35) of $t_{1/2}$ for RSA. Using an estimate for the exchangeable albumin pool size (270 mg albumin/100 g body wt) (18), we calculated the absolute rate of albumin synthesis to be 5.2 mg/h/100 g body wt in fed rats. Results of others in normal, fed rats reported using different methods have been variable but generally similar (19–24).

The coefficient of variation (C.V.) of the MIDA method was calculated from replicate analysis of the isotopomer pattern for individual rats. The average C.V. of the precursor measurement was 1.21% and ranged from 0.5 to 2.45% with a median of 0.95%. The average C.V. of the half-life value was 3.39% with a range of 0.77–8.92% and a median value of 1.94%. Thus, kinetic estimates by MIDA were reproducible under the experimental conditions tested here.

Some features of the method deserve comment. MIDA is based on the assumption of a single precursor pool enrichment. Possible temporal or regional differences in the precursor pool enrichment would not be detected by this method; rather, an average enrichment of the precursor would be estimated. We have previously demonstrated that the effect of differentially enriched pools on measures of f is minimal unless the isotopic gradient is very large (11, 15). Also, we

TABLE 7

Precursor Pool Enrichment and RSA Biosynthetic Parameters in Rats Fed *ad Libitum* (n = 7)

Precursor pool enrichment	f (day^{-1})	k_s (day^{-1})	$t_{1/2}$ (days)
0.390 ± 0.32	0.368 ± 0.018	0.463 ± 0.025	1.53 ± 0.09

Note. The value for f is expressed as a fraction per 24 h. Values shown are means ± SE.

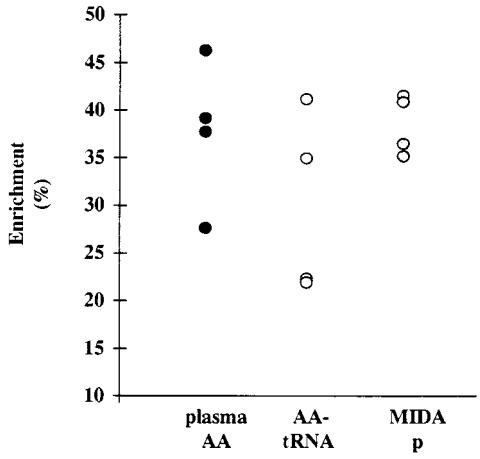

FIG. 5. Comparison of plasma, liver tRNA leucine, and MIDA-derived precursor enrichments ($n = 4$ in each group).

chose here to study relatively high precursor pool enrichments (30–40%) to increase isotopomeric abundances and reduce analytic error. Accordingly, the method described here is not a true "tracer" technique. It should be noted, however, that plasma leucine values increase by more than two- to threefold in the fed state (25–27), so that the labeled leucyl-tRNA values of 30–40% represent a relatively small additional increase under fed conditions. In the fasted state, leucine pools might be increased by the labeled leucine administered. Future applications could in principle be carried out at values of p close to 15%, if there are concerns about nontracer effects.

In summary, analysis of the mass isotopomer distribution pattern of a polypeptide product that has been perturbed by incorporation of labeled amino acid subunits is shown to reveal the proportion of isotopically labeled subunits that were present in the precursor biosynthetic pool and the fractional biosynthetic contribution to the protein pool. This approach generated appropriate and reproducible estimates using both an *in vitro* synthesis model from known leucine enrichments and an *in vivo* model in the rat. The enrichment of the precursor pool was closely approximated by analysis of the peptide's isotopomer pattern, acquired using either a magnetic sector or a quadrupole mass analyzer. Although relatively high precursor pool enrichments were tested here, these results confirm that the MIDA approach works both in principle and in practice and is suitable for measuring protein synthesis *in vivo*.

APPENDIX

When all the ions in the mass isotopomer spectrum are not monitored, there is no effect on calculation of p, which can still be calculated uniquely from ratios of measured isotopomers, using the look-up table. An effect on f will be observed, however, unless the calculation algorithm is corrected for the relative proportions of ions from the labeled and unlabeled populations that are sampled. Because of unequal molar contributions to the ion spectrum in the mixture, a mole of natural abundance molecules will be overrepresented in the envelope sampled relative to a mole of enriched molecules (i.e., there are fewer "diluting" ions in the enriched molecular population) and the assumption of linearity for mixtures no longer applies. It is therefore necessary to weight the contributions from the different populations. A simple algebraic correction can be formulated (17):

If $R_{(B)}$ Is the ratio or proportion of ions out of the total envelope that are monitored (at baseline), $R_{(E)}$ Is the ratio or proportion of ions out of the total envelope that are monitored (for enriched molecules), $M_{1(meas)}$ is the measured M_1 fractional abundances within the spectrum sampled from the mixture at the value of p calculated, $M_{1(B)}$ is the theoretical fractional abundance of M_1 ions within the total envelope (at baseline), and $M_{1(E)}$ is the theoretical fractional abundance of M_1 ions within the total envelope (for enriched molecules at the value of p calculated), then

$$f = \frac{[R_{(B)} \times M_{1(meas)}] - [M_{1(B)}]}{[M_{1(E)} - M_{1(B)}] + [(R_{(B)} - R_{(E)}) \times M_{1(meas)}]}.$$

The derivation is

$$M_{1(meas)} = \frac{[f \cdot M_{1(E)}] + [(1 - f) \times M_{1(B)}]}{f \cdot (R_E - R_B) + R_B}$$

$$= \frac{f(M_{1(E)} - M_{1(B)}) + M_{1(B)}}{f(R_E - R_B) + R_B}$$

$$f(R_E - R_B) + R_B = \frac{f[M_{1(E)} - M_{1(B)}]}{M_{1(meas)}} + \frac{M_{1(B)}}{M_{1(meas)}}$$

$$f\left[(R_E - R_B) - \left(\frac{M_{1(E)} - M_{1(B)}}{M_{1(meas)}} \right) \right] = \left[\frac{M_{1(B)}}{M_{1(meas)}} - R_B \right]$$

$$f = \frac{R_B - \frac{M_{1(B)}}{M_{1(meas)}}}{\left[\frac{M_{1(E)} - M_{1(B)}}{M_{1(meas)}} \right] - (R_E - R_B)}$$

$$= \frac{[R_B \cdot M_{1(meas)}] - M_{1(B)}}{[M_{1(E)} - M_{1(B)}] + [(R_B - R_E) \times M_{1(meas)}]}.$$

When $R_{(E)} = R_{(B)} = 1.0$ (i.e., all ions are monitored, for both populations), the equation reduces to

$$f = \frac{M_{1(\text{meas})} - M_{1(B)}}{M_{1(E)} - M_{1(B)}} = \frac{\Delta A_1(\text{mixture})}{\Delta A_1^*}.$$

Therefore, the equation reduces to the standard form (Eq. [1]), as it should, when the complete ion spectrum is monitored.

REFERENCES

1. Schoenheimer, R. (1942) *The Dynamic State of Body Constituents,* Harvard Univ. Press, Cambridge, MA.
2. Waterlow, J. C., Garlick, P. J., and Millward, D. J. (1978) Protein Turnover in Mammalian Tissues and in the Whole Body, North-Holland, Amsterdam/New York/Oxford.
3. Rennie, M. J., Smith, K., and Watt, P. W. (1994) *Am. J. Physiol.* **266,** E298–E307.
4. Nair, K. S. (Ed.) (1992) Protein Synthesis in Diabetes Mellitus, Smith-Gordon/Nishimura, London.
5. Baumann, P. Q., Stirewalt, W. S., O'Rourke, B. D., Howard, D., and Nair, K. S. (1994) *Am. J. Physiol.* **267,** E203–E209.
6. Airhart, J., Vidrich, A., and Khairallah, E. A. (1974) *Biochem. J.* **140,** 539–545.
7. Khairallah, E. A., Airhart, J., Bruno, M. K., Puchalsky, D., and Khairallah, L. (1977) *Acta. Biol. Med. Ger.* **36,** 1735–1745.
8. Garlick, P. J., McNurlan, M. A., Essen, P., and Wernerman, J. (1994) *Am. J. Physiol.* **266,** E287–E297.
9. Fern, E. B., and Garlick, P. J. (1976) *Biochem. J.* **156,** 189–192.
10. Ilan, J., and Singer, M. (1975) *J. Mol. Biol.* **91,** 39–51.
11. Hellerstein, M. K., and Neese, R. A. (1992) *Am. J. Physiol.* **263,** E988–E1001.
12. Hellerstein, M. K., Christiansen, M., Kaempfer, S., Kletke, C., Wu, K., Reid, J. S., Hellerstein, N. S., and Shackleton. C. H. L. (1991) *J. Clin. Invest.* **87,** 1841–1852.
13. Hellerstein, M. K., Wu, K., Kaempfer, S., Kletke, C., and Shackleton, C. H. L. (1991). *J. Biol. Chem.* **266,** 10912–10919.
14. Faix, D., Neese, R. A., Kletke, C., Walden, S., Cesar, D., Coutlangus, M., Shackleton, C. H. L., and Hellerstein, M. K. (1993) *J. Lipid Res.* **34,** 2063—2075.
15. Neese, R. A., Schwarz, J. M., Faix, D., Turner, S., Letscher, A., Vu, D., and Hellerstein, M. K. (1995) *J. Biol. Chem.* **270,** 14452–14466, and Hellerstein, M. K. (1991) *J. Biol. Chem.* **266,** 10920–10924.
16. Darnell, J., Lodish, H., and Baltimore, D. (1990) Molecular Cell Biology, Scientific American Books, New York.
17. Hellerstein, M. K., and Neese, R. A. Submitted for publication.
18. Jeffay, H., and Winzler, R. J. (1958) *J. Biol. Chem.* **231,** 111–116.
19. Katz, J., Bonorris, G., and Sellers, A. L. (1963) *J. Lab. Clin. Med.* **62**(6), 910–934.
20. Weigle, W. O. (1957) *PSEBM* **94,** 306–309.
21. Sellers, A. L., Katz, J., Bonorris, G., and Okuyama, S. (1966) *J. Lab. Clin. Med.* **68**(2), 177–185.
22. Morgan, E. H., and Peters, T., Jr. (1971) *J. Biol. Chem.* **246**(11), 3500–3507.
23. Peters, T., Jr., and Peters, J. C. (1972) *J. Biol. Chem.* **247**(12), 3858–3863.
24. Haider, M., and Tarver, H. (1969) *J. Nutr.* **99,** 433–445.
25. Tannous, R., Rogers, Q., and Harper, A. (1966) *Arch. Biochem. Biophys.* **113,** 356–361.
26. Clark, A., Umezawa, C., and Swendseid, M. (1973) *Am. J. Clin. Nutr.* **26,** 1175–1179.
27. Ashley, D., Barclay, D., Chauffard, F., Moennoz, D., and Leathwood, P. (1982) *Am. J. Clin. Nutr.* **36,** 143–153.